


Article

Internalization of Titanium Dioxide Nanoparticles Is Cytotoxic for H9c2 Rat Cardiomyoblasts

Elizabeth Huerta-García ¹, Iván Zepeda-Quiroz ¹, Helen Sánchez-Barrera ¹, Zaira Colín-Val ¹, Ernesto Alfaro-Moreno ², María del Pilar Ramos-Godínez ³ and Rebeca López-Marure ^{1,*} 

¹ Departamento de Fisiología (Biología Celular), Instituto Nacional de Cardiología “Ignacio Chávez”, Juan Badiano No. 1, Colonia Sección XVI, Tlalpan, C.P. 14080, Ciudad de México, Mexico; marlon_32001@yahoo.com.mx (E.H.-G.); poke_621@hotmail.com (I.Z.-Q.); helenisimasab@gmail.com (H.S.-B.); zaira.cv.10@gmail.com (Z.C.-V.)

² Swetox, Karolinska Institutet, Unit of Toxicology Sciences, Forskargatan 20, SE-151 36 Södertälje, Sweden; ernesto.alfaro-moreno@swetox.se

³ Departamento de Microscopía Electrónica, Instituto Nacional de Cancerología, Av. San Fernando No. 22, Colonia Sección XVI, Tlalpan, C.P. 14080 Ciudad de México, Mexico; pilyrg@gmail.com

* Correspondence: rlmare@yahoo.com.mx; Tel.: +52-55-55732911 (ext. 25401)

Received: 29 June 2018; Accepted: 1 August 2018; Published: 6 August 2018



Abstract: Titanium dioxide nanoparticles (TiO₂ NPs) are widely used in industry and daily life. TiO₂ NPs can penetrate into the body, translocate from the lungs into the circulation and come into contact with cardiac cells. In this work, we evaluated the toxicity of TiO₂ NPs on H9c2 rat cardiomyoblasts. Internalization of TiO₂ NPs and their effect on cell proliferation, viability, oxidative stress and cell death were assessed, as well as cell cycle alterations. Cellular uptake of TiO₂ NPs reduced metabolic activity and cell proliferation and increased oxidative stress by 19-fold measured as H₂DCFDA oxidation. TiO₂ NPs disrupted the plasmatic membrane integrity and decreased the mitochondrial membrane potential. These cytotoxic effects were related with changes in the distribution of cell cycle phases resulting in necrotic death and autophagy. These findings suggest that TiO₂ NPs exposure represents a potential health risk, particularly in the development of cardiovascular diseases via oxidative stress and cell death.

Keywords: titanium dioxide nanoparticles; cardiomyoblasts; internalization; oxidative stress; necrosis; autophagy

1. Introduction

Titanium dioxide nanoparticles (TiO₂ NPs) are widely used in foods, medicines, and cosmetics [1]. Human exposure occurs either by oral, dermal or inhalation routes [2]. Although initially considered safe and inert, TiO₂ NPs may actually be harmful for human health. For example, mice exposed to TiO₂ NPs developed strong pulmonary inflammation, acute phase responses and cytokine release into circulation [3]. In mice instilled intratracheally with low (18 µg) and high (162 µg) TiO₂ NPs doses, these nanoparticles were accumulated in heart and liver and translocated into circulation 24 h after exposure [4]. TiO₂ NPs activated the complement cascade and inflammatory processes in the heart, and triggered early innate immune responses in blood mediated by the complement factor 3. In liver, TiO₂ NPs altered gene expression related to acute phase response [4]. Oral and intravenous administrations of various TiO₂ NPs resulted in accumulation in many organs including liver, lung and heart, regardless of particle size, crystalline form or hydrophobicity [5]. Furthermore, abdominal injection of TiO₂ NPs in mice caused titanium accumulation in several organs, seriously damaging the liver, kidneys and heart and altering blood sugar and lipids [6]. Taken together, these results suggest that TiO₂ NPs can accumulate in different organs producing tissue damage and inflammation.

Despite TiO₂ NPs have been described as an inert material [7], several studies have shown the opposite. In the cardiovascular system, several experiments *in vivo* have shown myocardial damage, oxidative stress, inflammation and atherosclerosis in mice exposed to TiO₂ NPs [6]. Daily gastrointestinal administration of TiO₂ NPs at 0, 2, 10, 50 mg/kg in rats for up to three months resulted in cardiac dysfunction and inflammatory response [7]. Intragastric feeding of mice with TiO₂ NPs for nine consecutive months resulted in their accumulation in the heart causing inflammation, apoptosis and cardiac dysfunction [8].

Other studies have shown a strong increase of reactive oxygen species (ROS). Sheng and collaborators [9] administered different doses (2.5, 5, 10 mg/kg body weight) of TiO₂ NPs for a long-term exposure (90 days) inducing oxidative stress and antioxidant system attenuation in mice heart. TiO₂ NPs accumulated in the heart causing sparse cardiac muscle fibers, inflammatory response, cell necrosis, and cardiac biochemical dysfunction. There was an increase of superoxide radicals, hydrogen peroxide, malondialdehyde, carbonyl and 8-OHdG, as well as degradation products of proteins, lipids and DNA oxidation [9]. Overall, cell toxicity induced by nanoparticles has been associated to induction of oxidative stress. One study showed that macrophage-like THP-1 and HPMEC-ST1.6R microvascular cells exposed to TiO₂ NPs were sensitive to endogenous redox changes and apoptosis [10,11]. A549 cells incubated with TiO₂ NPs (Anatase 22.1 nm) for 24 h showed reduced cell viability and increased lactate dehydrogenase activity in a concentration-dependent manner, indicating cell membrane damage [12]. Also murine microglial cells (BV-2) treated at different concentrations of TiO₂ NPs (0.1 to 200 µg/mL) showed a slight inhibition of cell growth. High TiO₂ NPs concentrations enhanced permeability of cytoplasmic membrane to propidium iodide (PI), associated with loss of mitochondrial membrane potential ($\Delta\Psi_m$) and overproduction of superoxide anions [13]. In primary rat cortical astrocytes and human lung fibroblast cells (WI-38), TiO₂ NPs induced ROS generation and reduced $\Delta\Psi_m$ [14]. Moreover, food grade TiO₂ NPs promoted intracellular oxidative stress in WI-38 cells, altering cell cycle progression (G2/M > S > G0/G1) [15].

Many studies have described negative effects of TiO₂ NPs in various systems and cell types [2,11]. In the cardiovascular system, these nanoparticles induce tissue damage and inflammatory responses; however, the underlying mechanisms are not well understood. Therefore, in order to assess the impact of TiO₂ NPs on cardiac cells we evaluated their cellular uptake in H9c2 rat cardiomyoblasts and the mechanisms associated with their nanotoxicity.

Since TiO₂ NPs can translocate into the systemic circulation and the heart [4], we hypothesized that these nanoparticles could induce damage to cardiac cells. To test this hypothesis, we exposed H9c2 cells to TiO₂ NPs and examined their effects on cell cycle phases, mitochondrial function, oxidative stress, cell death and autophagy.

2. Results

2.1. Internalization of TiO₂ NPs

Due to their small size, nanoparticles uptake can occur in cardiac cells. In order to corroborate this, H9c2 cells were exposed to 5 µg/cm² TiO₂ NPs for 24 h and were then analyzed by transmission electron microscopy (TEM). Numerous nanoparticle aggregates with size < 500 nm were observed inside cells (Figure 1B); however, large aggregates > 2 µM were also present (Figure 1C,D). Internalized TiO₂ NPs were localized in the cytoplasm but solid core NPs were not observed inside cell organelles.

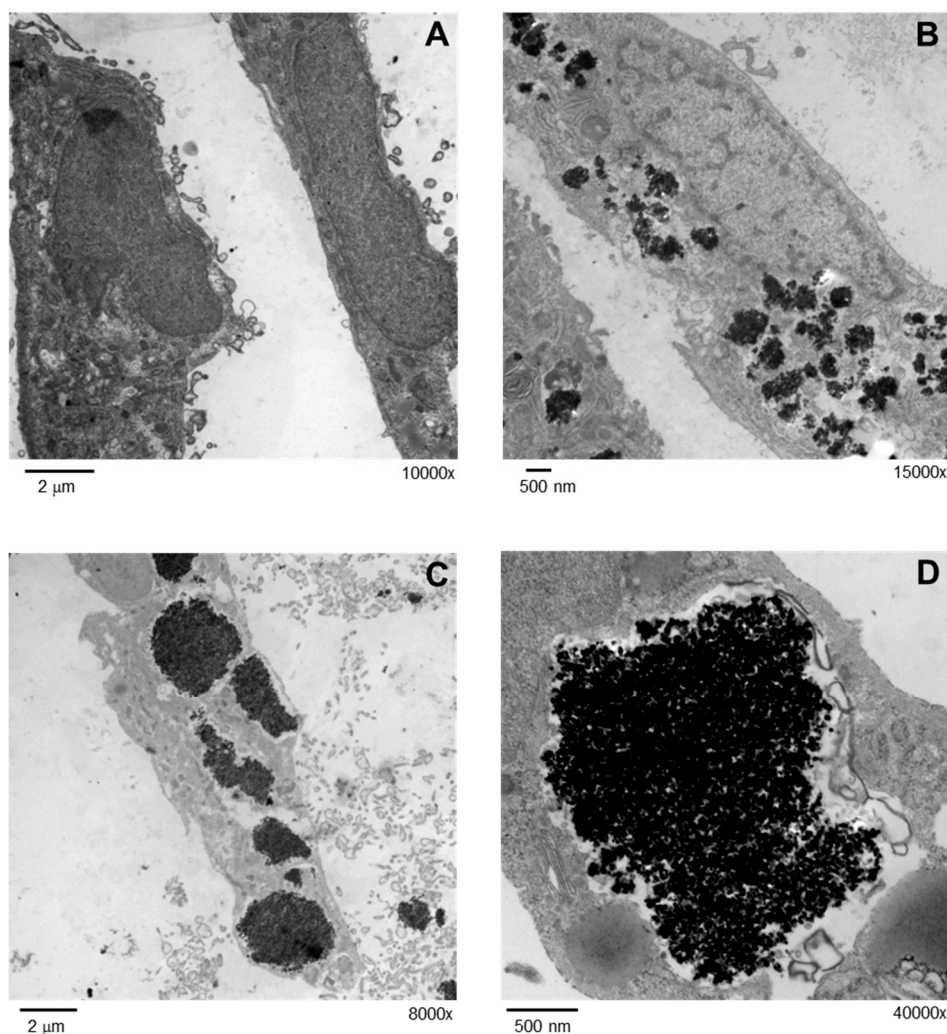


Figure 1. Internalization of TiO₂ NPs was evaluated by TEM. Cells were treated with 5 μg/cm² TiO₂ NPs for 24 h and analyzed in a JEOL 10-10 microscope and an AMT Camera System. TEM micrographs of non-exposed cells at a direct magnification of 10,000× (A) and treated cells a magnification of 15,000× (B), 8000× (C) and 40,000× (D) are shown.

2.2. TiO₂ NPs Inhibited Proliferation and Decreased Metabolic Activity

Large TiO₂ NPs aggregates observed inside cells could induce cytostatic/cytotoxic effects, therefore we evaluated their impact on cell proliferation and viability. To measure proliferation, H9c2 cells were exposed to different TiO₂ NPs concentrations for 72 h and were stained with crystal violet. Results showed that high NPs concentrations (20 and 40 μg/cm²) decreased cell proliferation in about 30% ($p < 0.05$ versus control cells) (Figure 2A). To evaluate viability, a MTT assay was performed. The metabolic activity was measured by MTT reduction to purple formazan by mitochondrial dehydrogenases in living cells. TiO₂ NPs from 5 μg/cm² decreased cell metabolic activity by 30%, and the maximum effect was achieved at 40 μg/cm² with 60% inhibition, compared to control cells (Figure 2B). The half maximal inhibitory concentration (IC₅₀) was 20 μg/cm² (100 μg/mL); therefore, further experiments in H9c2 cells were performed at this concentration.

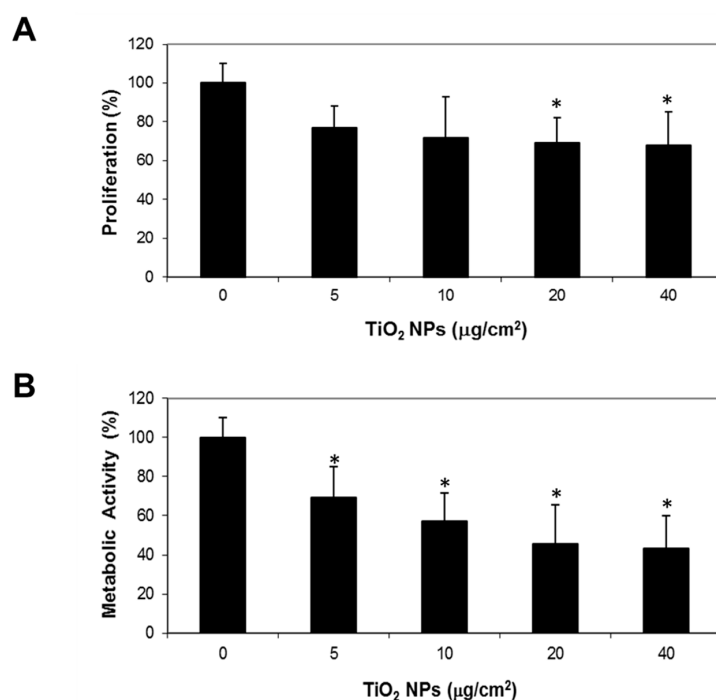


Figure 2. TiO₂ NPs treatment inhibited cell proliferation and decreased metabolic activity. H9c2 cells were treated with different TiO₂ NPs concentrations (5, 10, 20, 40 µg/cm²) for 48 h. Cell proliferation was evaluated by crystal violet staining and viability by MTT reduction. Results were expressed as mean ± standard deviation (SD) of three independent experiments ($n = 15$). * Significant difference between control (untreated) and treated cells ($p < 0.05$).

2.3. TiO₂ NPs Changed Cellular Redox State

TiO₂ NPs diminished cell viability and this cytotoxic effect is generally associated with oxidative stress. Therefore, we measured cellular redox state and ROS production by 2',7'-dichlorodihydrofluorescein diacetate (H₂DCFDA) oxidation. Results showed that TiO₂ NPs strongly increased the fluorescence intensity in direct proportion to H₂DCFDA oxidation. This increment was observed at all evaluated times; however, the highest effect was obtained at day one of treatment with a 17-fold increase ($p > 0.05$) vs. control cells (Figure 3).

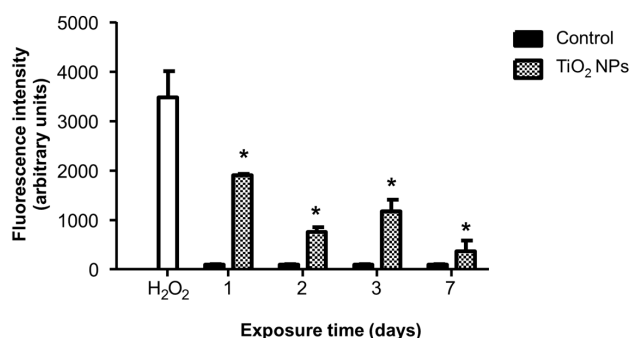


Figure 3. TiO₂ NPs treatment changed cellular redox state. H9c2 cells were treated with TiO₂ NPs (20 µg/cm²) alone for 1, 2, 3, and 7 days and cellular redox state was evaluated by H₂DCFDA oxidation. Cells treated with H₂O₂ (500 µM) for 1 day were used as positive controls. Results were expressed as fluorescence intensity in arbitrary units and as mean ± standard deviation (SD) of three independent experiments ($n = 15$). * Significant difference between control (untreated) and treated cells ($p < 0.05$).

2.4. TiO₂ NPs Decreased the Mitochondrial Membrane Potential

Oxidative stress was measured by changes in the $\Delta\Psi_m$ with rhodamine 123 (Rh123). This molecule is cell membrane permeable and localizes in the mitochondria of viable cells, but when the $\Delta\Psi_m$ is altered, Rh123 is released and the fluorescence intensity decreases. TiO₂ NPs decreased the fluorescence by 50% with a significant statistical difference from 48 h of treatment, indicating alterations in the $\Delta\Psi_m$ (Figure 4).

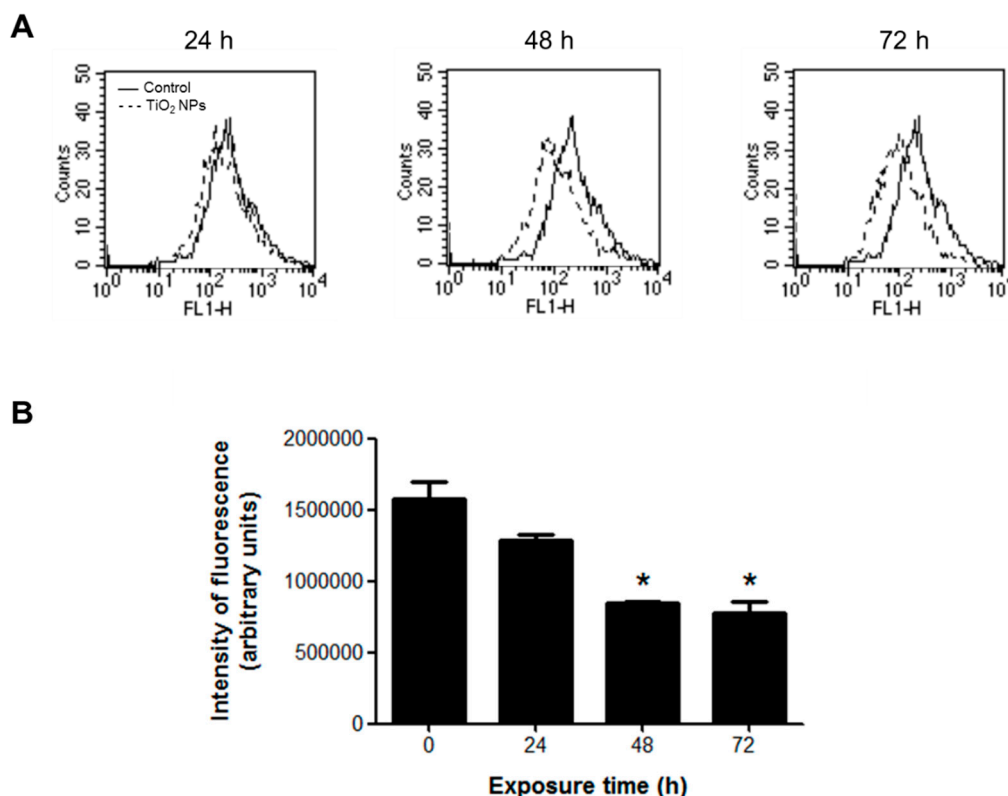


Figure 4. TiO₂ NPs decreased $\Delta\Psi_m$ in H9c2 cells treated with 20 $\mu\text{g}/\text{cm}^2$ TiO₂ NPs for 24, 48, and 72 h. $\Delta\Psi_m$ changes were measured by the fluorescent dye Rh123 in a flow cytometer. (A) Histograms of a representative experiment performed independently. (B) Densitometric analysis expressed as fluorescence intensity (arbitrary units). Data are presented as mean \pm standard deviation (SD) of three independent experiments ($n = 3$). * Significant difference between control (untreated) and treated cells ($p < 0.05$).

2.5. TiO₂ NPs Altered Cell Cycle Phases

To determine whether the effect of TiO₂ NPs on cell proliferation and viability was associated with cell cycle alterations, H9c2 cells were exposed to 20 $\mu\text{g}/\text{cm}^2$ TiO₂ NPs for 24, 48 and 72 h and the cell cycle phases were evaluated. The number of cells in the G1 phase decreased by 22% after 48 h of treatment and reached 34% at 72 h compared with control cells. No significant changes were observed in the S and G2/M phases in the same periods. The percentages of sub G1 cells significantly increased in a time-dependent manner, and peaked at 72 h with 39.9%. These results indicate that NPs caused important changes in the distribution of cell cycle phases after 48 h of exposure (Figure 5).

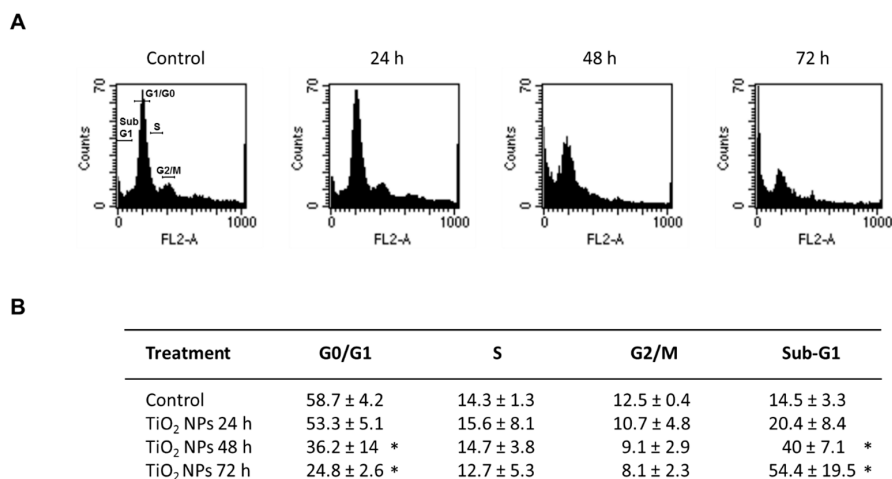


Figure 5. Effect of TiO₂ NPs on cell cycle. H9c2 cells were treated with 20 µg/cm² TiO₂ NPs for 24, 48, and 72 h and cell cycle was analyzed by quantitation of DNA content through flow cytometry. Histograms (A) and table (B) show the percentage of cell populations in each phase. In (B), data were analyzed by the CellQuest Pro software (Becton Dickinson) and expressed as mean ± standard deviation (SD) of three independent experiments ($n = 3$). * Significant difference between control (untreated) and treated cells ($p < 0.05$).

2.6. TiO₂ NPs Induced Necrotic Death and Autophagy

Since TiO₂ NPs induced a significant increase in sub-G1 peak, we characterized the type of cell death. No significant change in apoptosis was observed with TiO₂ NPs at any time; however, TiO₂ NPs produced a slight but significant 20% increase in necrotic cell death after 24 h of treatment (Figure 6). This was consistent with higher LDH release (30%) ($p < 0.05$) at 24 and 48 h (Figure 7).

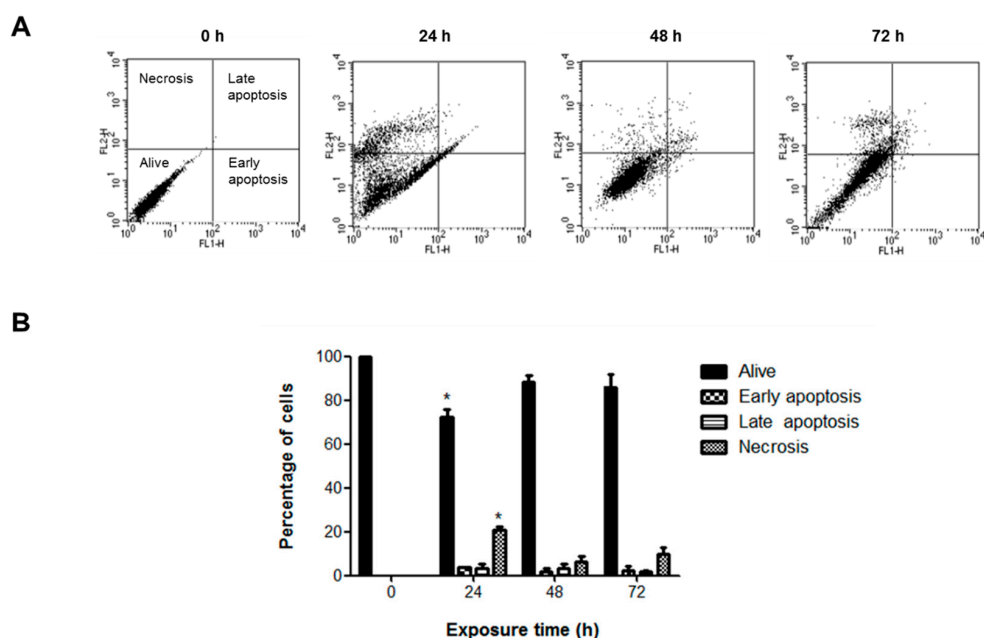


Figure 6. TiO₂ NPs induced necrotic death. H9c2 cells were treated with 20 µg/cm² TiO₂ NPs for 24, 48, and 72 h, then apoptotic and necrotic death was measured by annexin-V and propidium iodide staining. Dot plots show resolution of live, apoptotic and necrotic populations (A) and the bar chart show the percentages (B) as mean ± standard deviation (SD) of three independent experiments ($n = 3$). * Significant difference between control (untreated) and treated cells ($p < 0.05$).

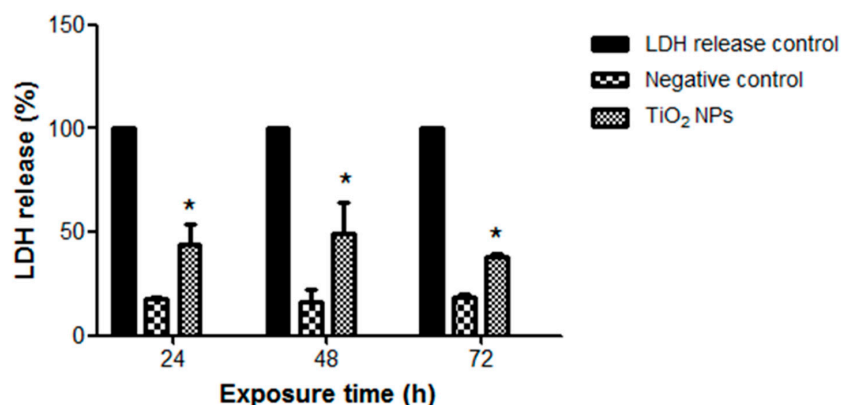


Figure 7. TiO₂ NPs induced LDH release. H9c2 cells were treated with 20 µg/cm² TiO₂ NPs for 24, 48, and 72 h and then an LDH-based cytotoxicity assay was performed. Results are presented as mean ± standard deviation (SD) of three independent experiments (*n* = 3). * Significant difference between negative control (untreated) and treated cells (*p* < 0.05).

TiO₂ NPs also induced strong morphological changes related to increased numbers of cell vacuoles (data not shown). Since autophagy is a self-degradative process and a survival mechanism involving generation of vacuoles [16], autophagic vesicles were detected using a novel and selective green fluorescent dye. TiO₂ NPs induced a nine-fold increase of fluorescence after 24 h of treatment, indicating the formation of autophagic vacuoles (Figure 8).

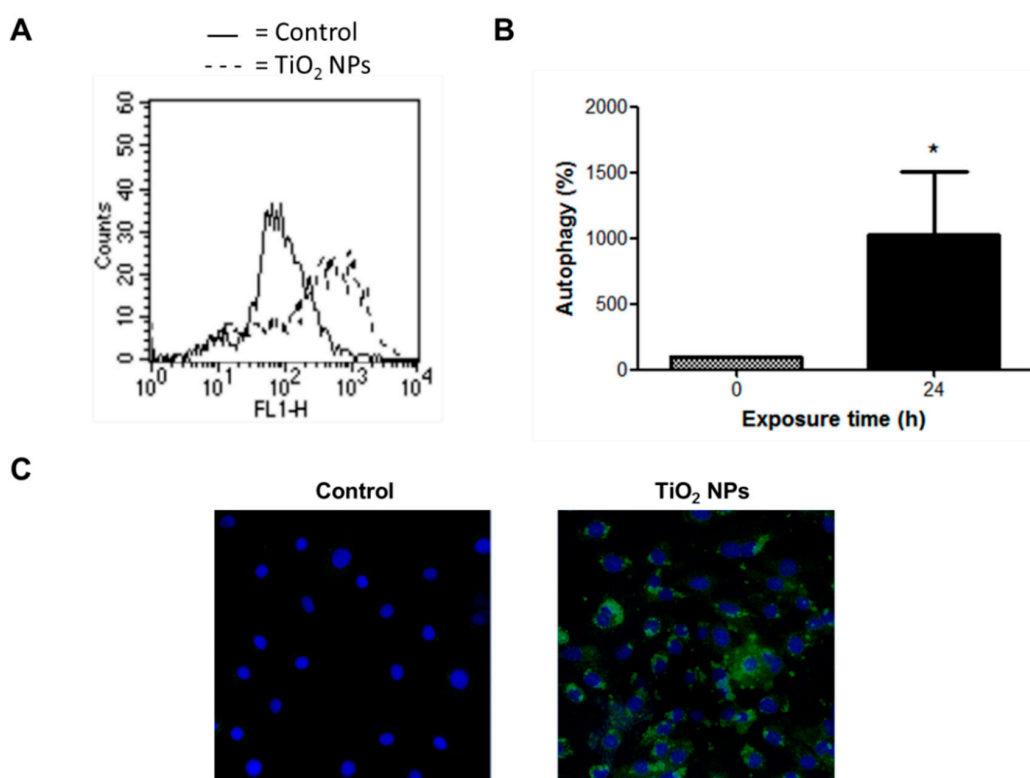


Figure 8. TiO₂ NPs induced autophagy. H9c2 cells were treated with 20 µg/cm² TiO₂ NPs for 24 h and autophagy was evaluated through a detection kit by flow cytometry (A,B) and confocal microscopy (C). In (B), results are presented as mean ± standard deviation (SD) of three independent experiments (*n* = 3). * Significant difference between untreated cells (0) and TiO₂ NPs-treated cells (*p* < 0.05). In (C), nuclear stain with DAPI and green detection reagent (autophagy) are showed.

3. Discussion

There is evidence that TiO₂ NPs can translocate to the heart via systemic circulation [4]. In this work we evaluated whether TiO₂ NPs could have adverse effects on cardiomyocytes, measured through cell viability, oxidative stress, $\Delta\Psi_m$, cell cycle and cell death.

TiO₂ NPs decreased cell proliferation and induced a strong cytotoxic effect on H9c2 cells, associated with increased oxidative stress and alterations of $\Delta\Psi_m$. Important changes in cell cycle phases were observed in association with necrotic death and autophagy. TiO₂ NPs also disrupted the integrity of cell membrane leading to increased permeability and LDH release (Figure 6).

Despite the fact TiO₂ NPs have been considered as inert and nontoxic, a growing body of evidence suggests quite the opposite. Cytotoxic effects of TiO₂ NPs are generally associated with cell growth inhibition in different cells types [13,17–22]; however, our results are the first evidence of their toxicity in cardiac H9c2 cells. The inhibitory concentration IC₅₀ was 20 $\mu\text{g}/\text{cm}^2$ (75 $\mu\text{g}/\text{mL}$), consistent with other in vitro studies [23]. Although this concentration of TiO₂ NPs is higher than those of occupational exposure or commercial products, TiO₂ NPs may accumulate by long-term exposure and become toxic. Particles of few nanometers in size can translocate through the air-blood-barrier in approximately 10% [24]. Considering that 40 $\mu\text{g}/\text{cm}^2$ of TiO₂ NPs could be present in hot-spots of airways and lungs of exposed humans [25], then approximately 4 $\mu\text{g}/\text{cm}^2$ could enter into systemic circulation. Once there, particles become highly diluted, but their bioaccumulation in different tissues is not well documented, therefore we hypothesized that these concentrations could be reached over long-term exposures. In a recent study, the biokinetics of 48 V-radiolabeled TiO₂ NPs was investigated in rats at retention time points 1, 4, 24 h and seven days after oral application of a single dose by intra-esophageal instillation. Their results showed that 0.6% of the administered dose passed the gastro-intestinal-barrier after one hour and about 0.05% was still distributed in the body after seven days, indicating the possibility of chronic accumulation of nanoparticles in secondary organs and the skeleton [26].

We observed internalization of TiO₂ NPs by H9c2 cells and these nanoparticles remained within cells even after cell division. Nanoparticles were accumulated in the cytoplasm but no interactions with organelles were observed (Figure 1). Chronic exposures at low concentrations of TiO₂ NPs in human bronchial epithelium cells (BEAS-2B) showed cellular uptake and cell transformation [27], supporting our observations. Few studies have analyzed the exocytosis of nanoparticles in mammalian cells. Wang et al. [28] showed that TiO₂ NPs were internalized by the neural stem cells after 48 h incubation, and only 35% was exocytosed after 24 h.

Nanoparticles interact directly with cells as complexes or aggregates [29]. The real identity and toxicity of TiO₂ NPs in biological systems is a function of surface charge, size, solubility, shape, hydrophobicity, dose and crystalline structures [30]. Nanoparticle surface becomes saturated by phospholipids, proteins, DNA, small molecules and inorganic ions. The nanoparticle surface ligand induces protein corona misfolding and therefore indirectly enhances cellular uptake [31].

TiO₂ reduction to nanosize increases surface area changing their electronic configuration and reactivity. These modifications also affect cell binding and internalization. The size of TiO₂ NPs aggregates in culture medium containing FBS is reduced, enhancing dispersion [32], facilitating contact with cells and toxicity.

Our results showed that TiO₂ NPs induced oxidative stress in H9c2 cells evidenced by changes in redox state (increased ROS production). After one day of exposure, TiO₂ NPs induced ROS generation but this declined after two days. A subsequent increase and decrease occurred at three and seven days, respectively. We hypothesize that after two days of treatment, the antioxidant defense system counteracts cell and mitochondrial damage, but after three days, cells lose this capacity. After seven days of exposure, the extent of cell damage is greater, making difficult to evaluate ROS production. TiO₂ NPs can produce ROS such as hydroxyl radicals and superoxides in the dark. These oxidize serum proteins to form a protein corona on the nanoparticles surface. This oxidized protein could be responsible for the oxidative stress induced by TiO₂ NPs in H9c2 cells [33]. In a previous experiment

performed in acellular conditions using a dithiothreitol (DTT) assay [34], we found the oxidant potential of TiO₂ NPs.

Oxidative stress appears to be the underlying mechanism of *in vivo* genotoxicity of titanium [35]. We previously showed that oxidative stress induced by TiO₂ NPs can upregulate early and late receptors for adhesion molecules on monocytes [36]. Taken together, these data indicate that oxidative stress plays an important role and could be the primary mechanism for TiO₂ NPs toxicity in cardiomyoblasts.

Oxidative stress was related with dissipation of $\Delta\Psi_m$ in H9c2 cells, indicating mitochondrial dysfunction. Similar results were observed in H9c2 cells exposed to platinum-coated TiO₂ NPs (Pt-TiO₂ NPs) [37]; and in primary astrocytes exposed to different types of TiO₂ NPs, altering mitochondrial morphology, ROS generation, and $\Delta\Psi_m$, suggesting mitochondrial damage [14]. Mitochondrial dysfunction leads to ROS overproduction, damage to cellular components and cell death, forming a vicious cycle [38].

Studies in yeast and complex eukaryotes show that fluctuations in oxygen consumption, energy metabolism, and cell redox state are intimately integrated with cell cycle progression [39]. Therefore, we evaluated cell cycle phases in H9c2 cells exposed to TiO₂ NPs. Our results showed that TiO₂ NPs induced changes in the cell cycle. The proportion of G0/G1 phase cells decreased and the percentage of sub-G1 region events increased after 48 and 72 h of exposure, associated with necrosis and autophagy. Different forms of TiO₂ NPs induced cell cycle arrest in various cells types [15,40,41], in connection with elevated ROS levels [40,42,43], indicating that cytotoxic effects of TiO₂ NPs are related to oxidative stress, cell cycle alterations and cell death.

H9c2 cells exposed to TiO₂ NPs had severe damage resulting in strong autophagy (Figure 8). Autophagy involves lysosomal degradation of cytoplasmic components such as mitochondria and other intra-cellular structures [44,45]. Autophagy increases following mitochondrial dysfunction such as generation of low ATP levels; therefore, mitochondria have a key role in autophagy [46]. Autophagy is implicated in tumor suppression through cell cycle arrest, promoting genome and organelle integrity, or through inhibition of necrosis-mediated inflammation [16]. Autophagy has also been linked to pathologic conditions of cardiac remodeling that involve an increase of cardiomyocyte death [47–50]. Autophagy observed in H9c2 cells may be a consequence of necrosis and inflammation induced by TiO₂ NPs in order to counteract the damage. In the heart autophagy can be either beneficial or harmful, but enhanced autophagy can induce cell death [51].

Some degree of necrosis but not apoptosis was observed in H9c2 cells exposed to TiO₂ NPs. Cardiomyocytes may undergo apoptosis, necrosis and autophagic death [52]. Necrosis and apoptotic cell death depend in part, on ATP levels. In situations where ATP depletion is extreme, apoptosis is inhibited and then necrosis might occur [52]. Necrosis may also result from acidosis and higher calcium concentrations. Nanoparticles possibly induced changes in ATP levels, acidosis or increased intracellular calcium levels resulting in necrotic death of H9c2 cells.

The mitochondrial intermembrane protein and activator of caspases is released from the intermembrane space following outer membrane rupture. ROS production and mitochondrial alterations induced by TiO₂ NPs in H9c2 cells may promote mitochondrial permeability transition and subsequent cell death. Cellular features of necrosis, apoptosis, and autophagy frequently co-occur after death signals and toxic stress [50]. Further studies are needed to evaluate whether long term exposure of cells to TiO₂ NPs produces autophagic death.

In summary, TiO₂ NPs cause severe damage to cardiomyoblasts cells *in vitro* through inhibition of proliferation (1), induction of oxidative stress and mitochondrial dysfunction (2, 3), autophagy (4), membrane permeability and necrotic death (5) (Figure 9), indicating that occupational and environmental exposures to these NPs, could eventually lead to heart damage and the development of cardiovascular diseases. Taken together, these results suggest that nanoparticles accumulation in cardiomyoblasts, could eventually drive cardiac damage and adverse health effects in the exposed population.

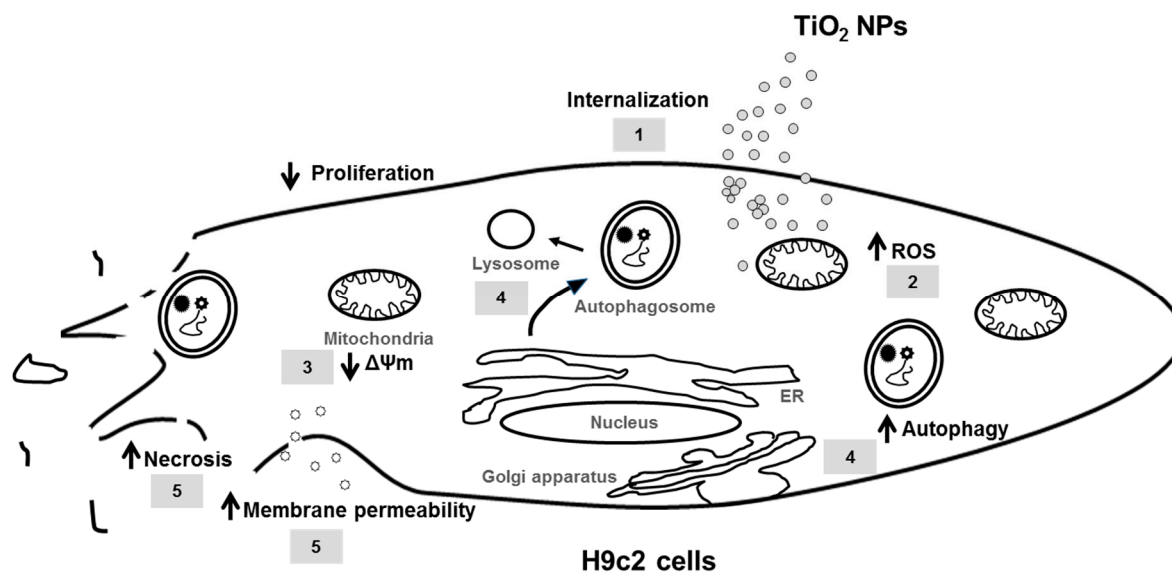


Figure 9. Toxic effects induced by TiO₂ NPs in H9c2 cells. TiO₂ NPs are internalized into the cytoplasm (1), producing strong oxidative stress and changes in the cellular redox state, increasing ROS production and mitochondrial damage (2), decreasing mitochondrial membrane potential ($\Delta\Psi_m$) (3). High oxidative stress causes strong cell damage, associated with autophagy (4), involving the formation of autophagosomes in the endoplasmic reticulum (ER), these in turn fuse with lysosomes to produce degradation of cytoplasmic components formed during cell damage. Finally, TiO₂ NPs increase membrane permeability and induce necrosis (5).

4. Methods

4.1. Materials

Dulbecco's modified Eagle's medium (DMEM) high glucose, 0.25% trypsin-EDTA solution, Antibiotic Antimycotic Solution (100 \times), and fetal bovine serum (FBS) were acquired from Gibco BRL (Grand Island, NY, USA). Cell culture consumables were purchased from Corning (Corning, NY, USA). Flow cytometry reagents were provided by Becton-Dickinson Immunocytometry Systems (San Jose, CA, USA). H₂DCFDA was purchased from Molecular Probes, Invitrogen (Carlsbad, CA, USA). CytoTox 96 Non-radioactive cytotoxicity assay was from Promega (Madison, WI, USA). Western blot reagents were from Bio-Rad (Hercules, CA, USA). Autophagy detection kit was purchased from abcam (Cambridge, MA, USA). Anatase TiO₂ NPs 25 nm and other chemicals were obtained from Sigma-Aldrich (St. Louis, MO, USA).

4.2. Culture of Embryonic Rat H9c2 Cardiomyoblast Cells

H9c2 rat cardiomyoblasts were used as a model since they mimic the hypertrophic responses of primary rat neonatal cardiomyocytes in vitro [53]. H9c2 cells were purchased from the American Type Culture Collection (CRL-1446, ATCC, Manassas, VA, USA) and cultured with DMEM high glucose added with 10% fetal bovine serum (FBS) plus an antibiotic-antimycotic solution. Cells were cultured at 37 °C in a humidified atmosphere of 5% CO₂.

4.3. Titanium Dioxide Nanoparticles

TiO₂ NPs were previously characterized by our group [54]. TiO₂ NPs have a surface area of 45–50 m²/g with average particle size of 19 nm and ζ -potential of –12 mV. TiO₂ NPs were endotoxin-free and pure, containing only oxygen and titanium [55]. Before use, TiO₂ NPs were suspended at 1 mg/mL, in a HEPES phosphate buffer solution (HPBS: 4.4 mM KCl, 150 mM NaCl, 12.2 mM glucose, 10.9 mM HEPES, pH 7.4) and were vortexed a high speed for 2 min [54]. In previous

studies, TiO₂ NPs induced different toxic effects in a range from 1 to 100 µg/cm². We also found that 40 µg/cm² TiO₂ NPs induced a strong cytotoxicity in other cells; therefore, in this work we tested concentrations equal or below this value (1, 5, 10, 20, 40 µg/cm², equivalent to 5, 25, 50, 100 and 200 µg/mL). Concentrations are presented as µg/cm² since TiO₂ NPs suspensions are unstable and precipitate.

4.4. Internalization of TiO₂ NPs

Cellular uptake of nanoparticles was evaluated by TEM as previously described by Huerta-García and collaborators [55]. Cells (200 × 10³/well) were treated with 5 µg/cm² TiO₂ NPs for 24 h. Then cells were fixed with 2.5% glutaraldehyde-formaldehyde in HPBS for 1 h. A second fixation was performed in 2% OsO₄ (1:1 in HPBS) for 1 h. Cells were gradually dehydrated with increasing ethanol concentrations and embedded in epoxy resin (Epon 812, Sigma-Aldrich, St. Louis, MO, USA). Ultrathin sections were stained with lead citrate and alcoholic uranyl acetate. Finally, cells were examined with a transmission electron microscope (JEOL 10/10, MA, USA).

4.5. Proliferation Assay

H9c2 cells (8 × 10³ cells/well) were exposed to different concentrations of TiO₂ NPs (5, 10, 20, 40 µg/cm²) and cell proliferation was evaluated by crystal violet staining after 72 h of treatment according to Márquez-Ramírez and collaborators [56].

4.6. Cell Viability

The reduction of 3-(4,5-dimethylthiazol-2-yl)-2,5-diphenyltetrazolium bromide (MTT) to water-insoluble formazan was used to evaluate cell viability. H9c2 cells (8 × 10³ cells/well) were exposed to different concentrations of TiO₂ NPs (5, 10, 20, 40 µg/cm²) for 72 h. After treatment, cells were incubated with 5 mg/mL MTT for 4 h and optical density at 570 nm was measured in a microplate spectrophotometer.

4.7. Oxidative Stress

The cellular redox state and oxidative stress were measured by oxidation of the H₂DCFDA (non-fluorescent) to 2',7'-dichlorofluorescein (DCF) (highly fluorescent). Changes in the ΔΨ_m were assessed as described by Huerta-García and collaborators [57] using rhodamine 123 (Rh123), a cell-permeant cationic compound captured by the active mitochondria. H9c2 cells (1 × 10⁶ cells/treatment) were exposed to 20 µg/cm² TiO₂ NPs for 24, 48 and 72 h. After treatment, cell suspensions were incubated with 10 µM H₂DCFDA or 0.2 µg/mL Rh123 for 30 min in the dark. Finally, cells were analyzed in a flow cytometer (Fascalibur, Becton Dickinson, Franklin Lakes, NJ, USA).

4.8. Cell Cycle Phases

Flow cytometry and staining with PI was performed to study cell cycle changes induced by TiO₂ NPs. We selected the optimal concentration of TiO₂ NPs for a significant reduction in cell proliferation. Therefore, H9c2 cells were exposed to 20 µg/cm² TiO₂ NPs for 24, 48 and 72 h. Then cells were fixed with 70% ethanol, washed with HPBS and incubated with RNase (50 U/mL) for 1 h at 37 °C. Finally, cells were stained with PI (200 µg/mL) and analyzed by flow cytometry.

4.9. Cell Death

Apoptotic and necrotic death were measured by Annexin-V/PI staining and analyzed by flow cytometry. Necrosis was also assessed by lactate dehydrogenase (LDH) release. H9c2 cells were cultured with 20 µg/cm² TiO₂ NPs for 24, 48 and 72 h, incubated with 100 µL of Annexin-V plus PI in the dark at 37 °C for 30 min and then examined in a flow cytometer. To evaluate LDH release, cells were cultured in phenol red-free DMEM medium and exposed to nanoparticles. After exposure, 50 µL

of the supernatant were mixed with 50 μL of the substrate mix and incubated in the dark at room temperature for 30 min. After incubation, 50 μL of stop solution were added and optical density was measured at 490 nm (OD_{490}). Data were normalized by subtracting average background of culture medium from experimental values. Percentage of cytotoxicity was calculated by the formula:

$$\text{Cytotoxicity (\%)} = \frac{\text{Experimental LDH release (OD}_{490}\text{)}}{\text{Maximum LDH release control (OD}_{490}\text{)}} \times 100$$

4.10. Autophagy

Autophagy was evaluated with a detection kit according to the manufacturer's instructions. Autophagic vesicles are detected with a 488 nm-excitable green fluorescent dye and co-localization with LC3, a specific autophagosome marker. Cells were exposed to 20 $\mu\text{g}/\text{cm}^2$ TiO_2 NPs for 24 h. After exposure, cells were trypsinized, centrifuged at 1000 rpm for 5 min, and washed with 1 \times assay buffer. Then cells were centrifuged and re-suspended in 250 μL of phenol red-free cell culture medium containing 5% FBS and incubated with 250 μL of diluted green stain solution for 30 min at room temperature in the dark. After incubation, cells were collected by centrifugation, washed with 1 \times assay buffer and analyzed in a flow cytometer. To analyze autophagy by confocal microscopy, cells were grown on coverslips. After treatment with TiO_2 NPs, medium was removed and cells were washed twice with 1 \times assay buffer. Then, cells were covered with 100 μL of microscopy dual detection reagent and incubated at 37 $^\circ\text{C}$ for 30 min in the dark. Then, cells were washed with 100 μL of 1 \times assay buffer, fixed with 4% formaldehyde and washed again three times. Finally, stained cells were analyzed with a model LSM 700 confocal microscope (Zeiss, Thornwood, NY, USA).

4.11. Statistical Analysis

Data are presented as mean \pm standard deviation (SD) of at least three independent experiments. Data were analyzed by one-way analysis of variance (ANOVA) followed by post-hoc Tukey's multiple comparison test, using GraphPad prism software version 5.01 (GraphPad Software La Jolla, CA, USA). Differences among groups were considered statistically significant at $p < 0.05$.

Author Contributions: Conceptualization, R.L.M. and E.H.G.; Methodology and Investigation, E.H.G., I.Z.Q., H.S.B. and Z.C.V.; Software, E.H.G. and Z.C.V.; Validation and Formal Analysis, M.P.R.G.; Resources, and Data Curation, R.L.M.; Writing—Original Draft Preparation, R.L.M.; Writing—Review & Editing, R.L.M. and E.A.M.; Visualization, R.L.M.; Supervision, E.A.M.; Project Administration, R.L.M.; Funding Acquisition, R.L.M.

Funding: This work was supported by CONACyT under grant number 182341.

Acknowledgments: We would like to thank Felipe Massó Rojas for his support with the confocal microscope and Giovanni Soca-Chafre for style and grammar corrections.

Conflicts of Interest: The authors declare no conflicts of interest.

References

1. Ranjan, S.; Dasgupta, N.; Srivastava, P.; Ramalingam, C. A spectroscopic study on interaction between bovine serum albumin and titanium dioxide nanoparticle synthesized from microwave-assisted hybrid chemical approach. *J. Photochem. Photobiol. B* **2016**, *161*, 472–481. [[CrossRef](#)] [[PubMed](#)]
2. Shakeel, M.; Jabeen, F.; Shabbir, S.; Asghar, M.S.; Khan, M.S.; Chaudhry, A.S. Toxicity of nano-titanium dioxide (TiO_2 -NP) through various routes of exposure: A review. *Biol. Trace Elem. Res.* **2016**, *172*, 1–36. [[CrossRef](#)] [[PubMed](#)]
3. Husain, M.; Saber, A.T.; Guo, C.; Jacobsen, N.R.; Jensen, K.A.; Yauk, C.L.; Williams, A.; Vogel, U.; Wallin, H.; Halappanavar, S. Pulmonary instillation of low doses of titanium dioxide nanoparticles in mice leads to particle retention and gene expression changes in the absence of inflammation. *Toxicol. Appl. Pharmacol.* **2013**, *269*, 250–262. [[CrossRef](#)] [[PubMed](#)]

4. Husain, M.; Wu, D.; Saber, A.T.; Decan, N.; Jacobsen, N.R.; Williams, A.; Yauk, C.L.; Wallin, H.; Vogel, U.; Halappanavar, S. Intratracheally instilled titanium dioxide nanoparticles translocate to heart and liver and activate complement cascade in the heart of C57BL/6 mice. *Nanotoxicology* **2015**, *9*, 1013–1022. [[CrossRef](#)] [[PubMed](#)]
5. Geraets, L.; Oomen, A.G.; Krystek, P.; Jacobsen, N.R.; Wallin, H.; Laurentie, M.; Verharen, H.W.; Brandon, E.F.; de Jong, W.H. Tissue distribution and elimination after oral and intravenous administration of different titanium dioxide nanoparticles in rats. *Part. Fibre Toxicol.* **2014**, *11*. [[CrossRef](#)] [[PubMed](#)]
6. Liu, H.; Ma, L.; Zhao, J.; Liu, J.; Yan, J.; Ruan, J.; Hong, F. Biochemical toxicity of nano-anatase TiO₂ particles in mice. *Biol. Trace Elem. Res.* **2009**, *129*, 70–80, Erratum in. *Biol. Trace Elem. Res.* **2009**, *129*, 170–180. [[CrossRef](#)] [[PubMed](#)]
7. Chen, Z.; Wang, Y.; Zhuo, L.; Chen, S.; Zhao, L.; Luan, X.; Wang, H.; Jia, G. Effect of titanium dioxide nanoparticles on the cardiovascular system after oral administration. *Toxicol. Lett.* **2015**, *239*, 123–130. [[CrossRef](#)] [[PubMed](#)]
8. Hong, F.; Wu, N.; Zhao, X.; Tian, Y.; Zhou, Y.; Chen, T.; Zhai, Y.; Ji, L. Titanium dioxide nanoparticle-induced dysfunction of cardiac hemodynamics is involved in cardiac inflammation in mice. *J. Biomed. Mater. Res. Part A* **2016**, *104*, 2917–2927. [[CrossRef](#)] [[PubMed](#)]
9. Sheng, L.; Wang, X.; Sang, X.; Ze, Y.; Zhao, X.; Liu, D.; Gui, S.; Sun, Q.; Cheng, J.; Cheng, Z.; et al. Cardiac oxidative damage in mice following exposure to nanoparticulate titanium dioxide. *J. Biomed. Mater. Res. Part A* **2013**, *101*, 3238–3246. [[CrossRef](#)] [[PubMed](#)]
10. Hanot-Roy, M.; Tubeuf, E.; Guilbert, A.; Bado-Nilles, A.; Vigneron, P.; Trouiller, B.; Braun, A.; Lacroix, G. Oxidative stress pathways involved in cytotoxicity and genotoxicity of titanium dioxide (TiO₂) nanoparticles on cells constitutive of alveolo-capillary barrier in vitro. *Toxicol. In Vitro* **2016**, *33*, 125–135. [[CrossRef](#)] [[PubMed](#)]
11. Zhang, X.; Li, W.; Yang, Z. Toxicology of nanosized titanium dioxide: An update. *Arch. Toxicol.* **2015**, *89*, 2207–2217. [[CrossRef](#)] [[PubMed](#)]
12. Bai, W.; Chen, Y.; Gao, A. Cross talk between poly(ADP-ribose) polymerase 1 methylation and oxidative stress involved in the toxic effect of anatase titanium dioxide nanoparticles. *Int. J. Nanomed.* **2015**, *10*, 5561–5569.
13. Rihane, N.; Nury, T.; M'rad, I.; El Mir, L.; Sakly, M.; Amara, S.; Lizard, G. Microglial cells (BV-2) internalize titanium dioxide (TiO₂) nanoparticles: Toxicity and cellular responses. *Environ. Sci. Pollut. Res. Int.* **2016**, *23*, 9690–9699. [[CrossRef](#)] [[PubMed](#)]
14. Wilson, C.L.; Natarajan, V.; Hayward, S.L.; Khalimonchuk, O.; Kidambi, S. Mitochondrial dysfunction and loss of glutamate uptake in primary astrocytes exposed to titanium dioxide nanoparticles. *Nanoscale* **2015**, *7*, 18477–18488. [[CrossRef](#)] [[PubMed](#)]
15. Periasamy, V.S.; Athinarayanan, J.; Al-Hadi, A.M.; Juhaimi, F.A.; Mahmoud, M.H.; Alshatwi, A.A. Identification of titanium dioxide nanoparticles in food products: Induce intracellular oxidative stress mediated by TNF and CYP1A genes in human lung fibroblast cells. *Environ. Toxicol. Pharmacol.* **2015**, *39*, 176–186. [[CrossRef](#)] [[PubMed](#)]
16. Glick, D.; Barth, S.; Macleod, K.F. Autophagy: Cellular and molecular mechanisms. *J. Pathol.* **2010**, *221*, 3–12. [[CrossRef](#)] [[PubMed](#)]
17. Wang, Y.; Cui, H.; Zhou, J.; Li, F.; Wang, J.; Chen, M.; Liu, Q. Cytotoxicity, DNA damage, and apoptosis induced by titanium dioxide nanoparticles in human non-small cell lung cancer A549 cells. *Environ. Sci. Pollut. Res. Int.* **2015**, *22*, 5519–5530. [[CrossRef](#)] [[PubMed](#)]
18. Armand, L.; Biola-Clier, M.; Bobyk, L.; Collin-Faure, V.; Diemer, H.; Strub, J.M.; Cianferani, S.; Dorsseleer Van, A.; Herlin-Boime, N.; Rabilloud, T.; et al. Molecular responses of alveolar epithelial A549 cells to chronic exposure to titanium dioxide nanoparticles: A proteomic view. *J. Proteom.* **2016**, *134*, 63–73. [[CrossRef](#)] [[PubMed](#)]
19. Acar, M.S.; Bulut, Z.B.; Ateş, A.; Nami, B.; Koçak, N.; Yıldız, B. Titanium dioxide nanoparticles induce cytotoxicity and reduce mitotic index in human amniotic fluid-derived cells. *Hum. Exp. Toxicol.* **2015**, *34*, 74–82. [[CrossRef](#)] [[PubMed](#)]
20. Hou, Y.; Cai, K.; Li, J.; Chen, X.; Lai, M.; Hu, Y.; Luo, Z.; Ding, X.; Xu, D. Effects of titanium nanoparticles on adhesion, migration, proliferation, and differentiation of mesenchymal stem cells. *Int. J. Nanomed.* **2013**, *8*, 3619–3630.

21. Wang, J.; Ma, J.; Dong, L.; Hou, Y.; Jia, X.; Niu, X.; Fan, Y. Effect of anatase TiO₂ nanoparticles on the growth of RSC-364 rat synovial cell. *J. Nanosci. Nanotechnol.* **2013**, *13*, 3874–3879. [[CrossRef](#)] [[PubMed](#)]
22. Takaki, K.; Higuchi, Y.; Hashii, M.; Ogino, C.; Shimizu, N. Induction of apoptosis associated with chromosomal DNA fragmentation and caspase-3 activation in leukemia L1210 cells by TiO₂ nanoparticles. *J. Biosci. Bioeng.* **2014**, *117*, 129–133. [[CrossRef](#)] [[PubMed](#)]
23. Shi, H.; Magaye, R.; Castranova, V.; Zhao, J. Titanium dioxide nanoparticles: A review of current toxicological data. *Part. Fibre Toxicol.* **2013**, *10*, 15. [[CrossRef](#)] [[PubMed](#)]
24. Kreyling, W.G.; Hirn, S.; Möller, W.; Schleh, C.; Wenk, A.; Celik, G.; Lipka, J.; Schäffler, M.; Haberl, N.; Johnston, B.D.; et al. Air-blood barrier translocation of tracheally instilled gold nanoparticles inversely depends on particle size. *ACS Nano* **2014**, *8*, 222–233. [[CrossRef](#)] [[PubMed](#)]
25. Alfaro-Moreno, E.; García-Cuellar, C.M.; De Vizcaya Ruiz, A.; Rojas-Bracho, L.; Osornio-Vargas, A. The cellular mechanisms behind particulate matter air pollution related health effects. In *Air Pollution: Health & Environmental Impacts*; Gurjar, B.R., Molina, L.T., Ojha, C.S.P., Eds.; Taylor & Francis: Abingdon, Oxford, UK, 2010; pp. 249–274.
26. Kreyling, W.G.; Holzwarth, U.; Schleh, C.; Kozempel, J.; Wenk, A.; Haberl, N.; Hirn, S.; Schäffler, M.; Lipka, J.; Semmler-Behnke, M.; et al. Quantitative biokinetics of titanium dioxide nanoparticles after oral application in rats: Part 2. *Nanotoxicology* **2017**, *11*, 443–453. [[CrossRef](#)] [[PubMed](#)]
27. Vales, G.; Rubio, L.; Marcos, R. Long-term exposures to low doses of titanium dioxide nanoparticles induce cell transformation, but not genotoxic damage in BEAS-2B cells. *Nanotoxicology* **2015**, *9*, 568–578. [[CrossRef](#)] [[PubMed](#)]
28. Wang, Y.; Wu, Q.; Sui, K.; Chen, X.X.; Fang, J.; Hu, X.; Wu, M.; Liu, Y. A quantitative study of exocytosis of titanium dioxide nanoparticles from neural stem cells. *Nanoscale* **2013**, *7*, 4737–4743. [[CrossRef](#)] [[PubMed](#)]
29. Walczyk, D.; Bombelli, F.B.; Monopoli, M.P.; Lynch, I.; Dawson, K.A.J. What the cell “sees” in bionanoscience. *J. Am. Chem. Soc.* **2010**, *132*, 5761–5768. [[CrossRef](#)] [[PubMed](#)]
30. Warheit, D.B.; Hoke, R.A.; Finlay, C.; Donner, E.M.; Reed, K.L.; Sayes, C.M. Development of a base set of toxicity tests using ultrafine TiO₂ particles as a component of nanoparticle risk management. *Toxicol. Lett.* **2007**, *171*, 99–110. [[CrossRef](#)] [[PubMed](#)]
31. Prapainop, K.; Witter, D.P.; Wentworth, P. A chemical approach for cell-specific targeting of nanomaterials: Small-molecule-initiated misfolding of nanoparticle corona proteins. *J. Am. Chem. Soc.* **2012**, *134*, 4100–4103. [[CrossRef](#)] [[PubMed](#)]
32. Allouni, Z.E.; Cimpan, M.R.; Høl, P.J.; Skodvin, T.; Gjerdet, N.R. Agglomeration and sedimentation of TiO₂ nanoparticles in cell culture medium. *Colloids Surf. B Biointerfaces* **2009**, *68*, 83–87. [[CrossRef](#)] [[PubMed](#)]
33. Jayaram, D.T.; Runa, S.; Kemp, M.L.; Payne, C.K. Nanoparticle-induced oxidation of corona proteins initiates an oxidative stress response in cells. *Nanoscale* **2017**, *9*, 7595–7601. [[CrossRef](#)] [[PubMed](#)]
34. Nicolas, J.; Jaafar, M.; Sepetdjian, E.; Saad, W.; Sioutas, C.; Shihadeh, A.; Saliba, N.A. Redox activity and chemical interactions of metal oxide nano- and micro-particles with dithiothreitol (DTT). *Environ. Sci. Process Impacts* **2015**, *17*, 1952–1958. [[CrossRef](#)] [[PubMed](#)]
35. El-Ghor, A.A.; Noshay, M.M.; Galal, A.; Mohamed, H.R. Normalization of nano-sized TiO₂-induced clastogenicity, genotoxicity and mutagenicity by chlorophyllin administration in mice brain, liver, and bone marrow cells. *Toxicol. Sci.* **2014**, *142*, 21–32. [[CrossRef](#)] [[PubMed](#)]
36. Rueda-Romero, C.; Hernández-Pérez, G.; Ramos-Godínez, P.; Vázquez-López, I.; Quintana-Belmares, R.O.; Huerta-García, E.; Stepien, E.; López-Marure, R.; Montiel-Dávalos, A.; Alfaro-Moreno, E. Titanium dioxide nanoparticles induce the expression of early and late receptors for adhesion molecules on monocytes. *Part. Fibre Toxicol.* **2016**, *13*, 36. [[CrossRef](#)] [[PubMed](#)]
37. Mallik, A.; Bryan, S.; Puukila, S.; Chen, A.; Khaper, N. Efficacy of Pt-modified TiO₂ nanoparticles in cardiac cells. *Exp. Clin. Cardiol.* **2011**, *6*, 6–10.
38. Wang, C.H.; Wu, S.B.; Wu, Y.T.; Wei, Y.H. Oxidative stress response elicited by mitochondrial dysfunction: Implication in the pathophysiology of aging. *Exp. Biol. Med.* **2013**, *238*, 450–460. [[CrossRef](#)] [[PubMed](#)]
39. Burhans, W.C.; Heintz, N.H. The cell cycle is a redox cycle: Linking phase-specific targets to cell fate. *Free Radic. Biol. Med.* **2009**, *47*, 1282–1293. [[CrossRef](#)] [[PubMed](#)]
40. Ahamed, M.; Khan, M.A.; Akhtar, M.J.; Alhadlaq, H.A.; Alshamsan, A. Role of Zn doping in oxidative stress mediated cytotoxicity of TiO₂ nanoparticles in human breast cancer MCF-7 cells. *Sci. Rep.* **2016**, *6*, 30196. [[CrossRef](#)] [[PubMed](#)]

41. Gao, X.; Wang, Y.; Peng, S.; Yue, B.; Fan, C.; Chen, W.; Li, X. Comparative toxicities of bismuth oxybromide and titanium dioxide exposure on human skin keratinocyte cells. *Chemosphere* **2015**, *135*, 83–93. [[CrossRef](#)] [[PubMed](#)]
42. Kansara, K.; Patel, P.; Shah, D.; Shukla, R.K.; Singh, S.; Kumar, A.; Dhawan, A. TiO₂ nanoparticles induce DNA double strand breaks and cell cycle arrest in human alveolar cells. *Environ. Mol. Mutagen.* **2015**, *56*, 204–217. [[CrossRef](#)] [[PubMed](#)]
43. Ramkumar, K.M.; Manjula, C.; Gnanakumar, G.; Kanjwal, M.A.; Sekar, T.V.; Paulmurugan, R.; Rajaguru, P. Oxidative stress-mediated cytotoxicity and apoptosis induction by TiO₂ nanofibers in HeLa cells. *Eur. J. Pharm. Biopharm.* **2012**, *81*, 324–333. [[CrossRef](#)] [[PubMed](#)]
44. Klionsky, D.J. The molecular machinery of autophagy: Unanswered questions. *J. Cell Sci.* **2005**, *118*, 7–18. [[CrossRef](#)] [[PubMed](#)]
45. Kim, I.; Rodriguez-Enriquez, S.; Lemasters, J.J. Selective degradation of mitochondria by mitophagy. *Arch. Biochem. Biophys.* **2007**, *462*, 245–253. [[CrossRef](#)] [[PubMed](#)]
46. Levine, B.; Yuan, J. Autophagy in cell death: An innocent convict? *J. Clin. Investig.* **2005**, *115*, 2679–2688. [[CrossRef](#)] [[PubMed](#)]
47. Knaapen, M.W.; Davies, M.J.; De, B.M.; Haven, A.J.; Martinet, W.; Kockx, M.M. Apoptotic versus autophagic cell death in heart failure. *Cardiovasc. Res.* **2001**, *51*, 304–312. [[CrossRef](#)]
48. Shimomura, H.; Terasaki, F.; Hayashi, T.; Kitaura, Y.; Isomura, T.; Suma, H. Autophagic degeneration as a possible mechanism of myocardial cell death in dilated cardiomyopathy. *Jpn. Circ. J.* **2001**, *65*, 965–968. [[CrossRef](#)] [[PubMed](#)]
49. Cao, D.J.; Gillette, T.G.; Hill, J.A. Cardiomyocyte autophagy: Remodeling, repairing and reconstructing the heart. *Curr. Hypertens. Rep.* **2009**, *11*, 406–411. [[CrossRef](#)] [[PubMed](#)]
50. Nishida, K.; Kyo, S.; Yamaguchi, O.; Sadoshima, J.; Otsu, K. The role of autophagy in the heart. *Cell Death Differ.* **2009**, *16*, 31–38. [[CrossRef](#)] [[PubMed](#)]
51. De Meyer, G.R.; Martinet, W. Autophagy in the cardiovascular system. *Biochim. Biophys. Acta* **2009**, *1793*, 485–495. [[CrossRef](#)] [[PubMed](#)]
52. Mani, K. Programmed cell death in cardiac myocytes: Strategies to maximize post-ischemic salvage. *Heart Fail. Rev.* **2008**, *13*, 193–209. [[CrossRef](#)] [[PubMed](#)]
53. Watkins, S.J.; Borthwick, G.M.; Arthure, H.M. The H9C2 cell line and primary neonatal cardiomyocyte cells show similar hypertrophic responses in vitro. *In Vitro Cell. Dev. Biol. Anim.* **2011**, *47*, 125–131. [[CrossRef](#)] [[PubMed](#)]
54. Montiel-Dávalos, A.; Ventura-Gallegos, J.L.; Alfaro-Moreno, E.; Soria-Castro, E.; García-Latorre, E.; Cabañas-Moreno, J.G.; Ramos-Godinez, M.P.; López-Marure, R. TiO₂ nanoparticles induce dysfunction and activation of human endothelial cells. *Chem. Res. Toxicol.* **2012**, *25*, 920–930. [[CrossRef](#)] [[PubMed](#)]
55. Huerta-García, E.; Márquez-Ramírez, S.G.; Ramos-Godinez, M.P.; López-Saavedra, A.; Herrera, L.A.; Parra, A.; Alfaro-Moreno, E.; Gómez, E.O.; López-Marure, R. Internalization of titanium dioxide nanoparticles by glial cells is given at short times and is mainly mediated by actin reorganization-dependent endocytosis. *Neurotoxicology* **2015**, *51*, 27–37. [[CrossRef](#)] [[PubMed](#)]
56. Márquez-Ramírez, S.G.; Delgado-Buenrostro, N.L.; Chirino, Y.I.; Iglesias, G.G.; López-Marure, R. Titanium dioxide nanoparticles inhibit proliferation and induce morphological changes and apoptosis in glial cells. *Toxicology* **2012**, *302*, 146–156. [[CrossRef](#)] [[PubMed](#)]
57. Huerta-García, E.; Pérez-Arizti, J.A.; Márquez-Ramírez, S.G.; Delgado-Buenrostro, N.L.; Chirino, Y.I.; Iglesias, G.G.; López-Marure, R. Titanium dioxide nanoparticles induce strong oxidative stress and mitochondrial damage in glial cells. *Free Radic. Biol. Med.* **2014**, *73*, 84–94. [[CrossRef](#)] [[PubMed](#)]

Sample Availability: Samples of all the compounds that we used in this work are available from the authors.



© 2018 by the authors. Licensee MDPI, Basel, Switzerland. This article is an open access article distributed under the terms and conditions of the Creative Commons Attribution (CC BY) license (<http://creativecommons.org/licenses/by/4.0/>).